

A&A manuscript no.
(will be inserted by hand later)

Your thesaurus codes are:
06(08.01.1; 08.03.02; 08.16.2)

ASTRONOMY
AND
ASTROPHYSICS

Chemical analysis of 8 recently discovered extra-solar planet host stars[★]

N.C. Santos¹, G. Israelian², and M. Mayor¹

¹ Observatoire de Genève, 51 ch. des Maillettes, CH-1290 Sauverny, Switzerland

² Instituto de Astrofísica de Canarias, E-38200 La Laguna, Tenerife, Spain

Received / Accepted

Abstract. We present the chemical analysis of a new set of stars known to harbor low mass companions, namely HD 1237, HD 52265, HD 82943, HD 83443, HD 169830, and HD 202206. In addition, we have also analyzed HD 13445 and HD 75289, already studied elsewhere. The abundances of C and α -elements O, S, Si, Ca and Ti are presented and discussed in the context of the metallicity distribution of the stars with extra-solar planets. We compare the metallicity distribution of stars with planets with the same distribution of field dwarfs. The results further confirm that stars with planets are over-abundant in [Fe/H].

Key words: stars: abundances – stars: chemically peculiar – planetary systems

1. Introduction

Before the discovery of the first extra-solar planet (Mayor & Queloz 1995), the constraints on the planetary formation models were confined to the Solar System example. Today more than 40 extra-solar planetary systems are known. These discoveries immediately opened new horizons to this field, but also brought a bunch of new questions and problems. In fact, the extra-solar planets found to date don't have much in common with our own solar system. Their physical characteristics were completely unexpected. Some of them, like the extreme proximity of some of the new planets to their “mother” stars are surprising and still defy current formation models. A review of the subject can be found in Marcy, Cochran & Mayor (1999).

One particular fact became evident soon after the first extra-solar planets were discovered. The metallicity of the stars with planets proved to be distinctively different from the one found in field single dwarfs, being very metal-rich (Gonzalez 1997, 1998). As the number of extra-solar

planets is increasing, this fact is becoming more and more sharp.

Recent work showed that the high metallicity of the stars with giant planets cannot be the result of stellar population effects (Gonzalez 1999). Furthermore, Gonzalez & Laws (2000) add more evidence for chemical anomalies in stars with planetary companions. Their study suggests that the anomalies not only involve the [Fe/H] index, but possibly also the ratios [Li/H], [C/H] and [N/H]. The observed correlations between the presence of planets and the existence of chemical anomalies represent the only known physical connection between their presence and a stellar photospheric parameter, and their study is thus of major importance.

In addition to the discovery of a planet around HD 1237 (Naef et al. 2000), the Geneva extra-solar planet search group recently announced the discovery of 8 new low-mass companions to solar type stars (all with masses below $\sim 15 M_{\text{Jup}}^1$). These new planets and brown-dwarfs are included in a volume-limited sample of dwarfs (Udry et al. 2000). In this paper we present and discuss the abundance analysis of the elements C, O, S, Ca, Ti, Fe, and Si in the new candidates, HD 1237, HD 52265, HD 82943, HD 83443, HD 169830, and HD 202206. Planets have also been discovered during the CORALIE survey around HD 13445 (Queloz et al. 2000) and HD 75289 (Udry et al. 2000). We also present a spectroscopic analysis of these two stars, already studied by Flynn & Morell (1997), and Gonzalez & Laws (2000), respectively. The other three recently announced candidates (HD 108147, HD 162020 and HD 168746) will be the subject of a future publication.

2. Observations and data reduction

The spectra were obtained during three separate runs, between January and April 2000, using the new 1.2-m Euler Swiss telescope at La Silla (ESO), Chile, equipped with the CORALIE echelle spectrograph. The resolving power ($\lambda/\Delta\lambda$) of the spectrograph is about 50 000, and the spectra cover the visible spectrum between 3800 and

Send offprint requests to: Nuno.Santos@obs.unige.ch

[★] Based on observations collected at the La Silla Observatory, ESO (Chile), with the echelle spectrograph CORALIE at the 1.2-m Euler Swiss telescope

¹ www.eso.org/outreach/press-rel/pr-2000/pr-13-00.html

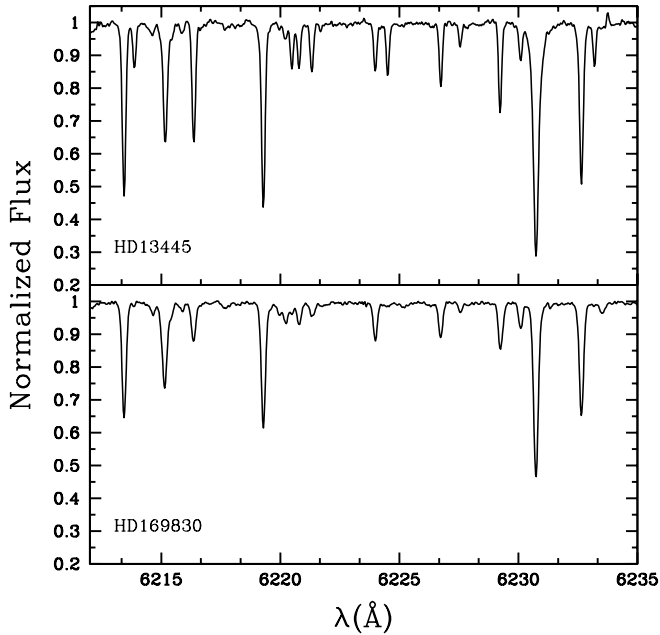


Fig. 1. Two sample CORALIE spectra of the K0 dwarf HD 13445 (upper panel), and of the F8 dwarf HD 169830 (lower panel).

6800 Å without gaps. The spectra have S/N ratios between about 150 and 350 (for the faintest objects we doubled the exposures). In Fig. 1 we present two sample spectra of HD 13445 and HD 169830.

The reduction of the spectra was carried out using standard tasks in the *echelle* package of IRAF². The wavelength calibration was done using the spectrum of a Thorium-Argon lamp that was taken in the beginning of the night.

After wavelength calibrated, the spectra were corrected for the radial-velocity Doppler shift using the velocity computed in the context of the planet search programme, and normalized using the CONTINUUM task in IRAF. In this step we divided the spectra into 350 Å wide intervals, that were normalized separately using 3rd order spline functions, and added together at the end. A visual inspection of the resulting spectra showed that the results were quite satisfactory.

3. Analysis

3.1. Spectrum Synthesis: Method

Abundance determination was done using a standard Local Thermodynamic Equilibrium (LTE) analysis with a revised version of the line abundance code MOOG (Sne-

den 1973), and a grid of Kurucz et al. (1993) ATLAS9 atmospheres.

Atomic data for iron lines was taken from the list of Gonzalez & Laws (2000). This choice was done so that our results would be in the same scale with theirs. Since we could not obtain a Solar spectrum, we also used the gf-values listed by these authors.

The line-lists for other elements were compiled from different authors, and semi-empirical gf-values were computed using equivalent widths obtained in the High Resolution Solar Atlas (Kurucz et al. 1984), and a solar model with $T_{\text{eff}} = 5777$ K, $\log g = 4.438$ and $\xi_t = 1$ km s⁻¹. We decided to adopt a value of $\log \epsilon_{\odot}(\text{Fe}) = 7.47$ (the same used by Gonzalez & Laws 2000). For other elements, the values were taken from Anders & Grevesse (1989).

Measured equivalent widths for the lines in the observed stars were determined by Gaussian fitting using the SPLIT task in IRAF. In Tables 1 and 2 we present the results, as well as the line parameters used ($\log gf$ and χ_l).

3.2. Stellar parameters and Abundances

Stellar atmospheric parameters were computed using the standard technique based on the Fe ionization balance. We first adopted initial atmospheric parameters computed from *ubvy*-photometry of Hauck & Mermilliod (1997) using the calibrations of Olsen (1984) for T_{eff} and $\log g$, Schuster & Nissen (1989) for [Fe/H] and Edvardsson et al. (1993) for ξ_t . Then, using the set of Fe I and Fe II lines presented in Table 1, we iterated until the correlation coefficients between $\log \epsilon(\text{Fe I})$ and χ_l , and between $\log \epsilon(\text{Fe I})$ and $\log (W_{\lambda}/\lambda)$ were zero (Fig. 2). The abundances derived from the Fe II lines were forced to be equal to those obtained from Fe I. The final atmospheric parameters, as well as the resulting iron abundances, are summarized in Table 3.

Errors in the parameters were estimated in the same way as in Gonzalez & Vanture (1998). The values were rounded to 25 K in T_{eff} , 0.05 dex in $\log g$, and 0.05 km s⁻¹ in ξ_t .

Uncertainties in the abundances of all elements were then determined adding the errors due to the sensitivities of the resulting abundances to changes of the atmospheric parameters (see Table 4 for two examples), and the dispersion of the abundances for the individual lines of each element. For elements with only one line measured, the errors only take into account the sensitivities to the atmospheric parameters. The dependence on ξ_t is always very small, and has no important implications in the final errors. The final abundance determinations and errors for C, O, S, Ca, Ti I, Ti II, and Si are presented in Table 5.

² IRAF is distributed by National Optical Astronomy Observatories, operated by the Association of Universities for Research in Astronomy, Inc., under contract with the National Science Foundation, U.S.A.

Table 1. Fe I and Fe II line parameters and measured equivalent widths.

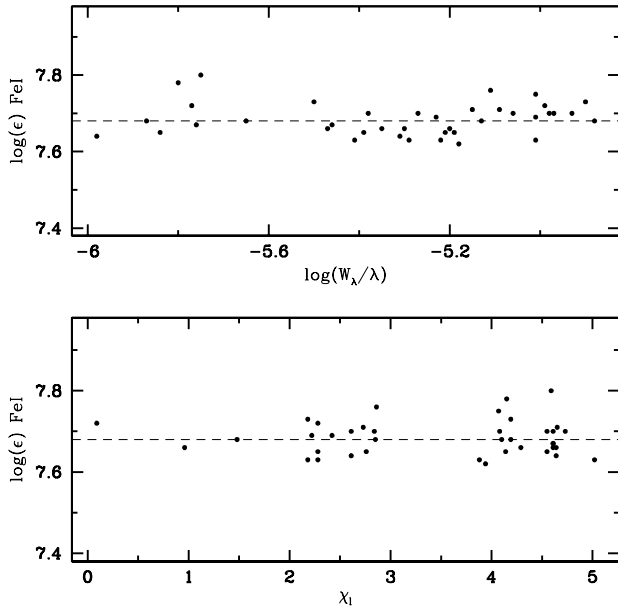
λ_0	χ_i	$\log gf$	HD 1237	HD 13445	HD 52265	HD 75289	HD 82943	HD 83443	HD 169830	HD 202206
Equivalent Widths (mÅ)										
Fe I	$\log \epsilon_{\odot} = 7.47$									
5044.21	2.85	-2.04	101.7	95.4	74.7	78.1	83.1	102.9	66.9	91.6
5247.05	0.09	-4.93	104.2	86.4	71.3	73.2	69.8	104.3	53.1	82.5
5322.05	2.28	-2.86	80.1	69.0	62.1	65.0	65.2	94.0	51.5	75.1
5806.73	4.61	-0.90	70.7	55.0	59.9	61.9	64.2	84.7	50.1	75.2
5852.22	4.55	-1.18	58.4	44.4	44.6	49.1	52.0	66.2	35.9	57.5
5855.09	4.61	-1.52	33.0	22.3	25.2	28.5	29.4	42.8	20.2	35.1
5856.09	4.29	-1.56	48.2	34.5	36.9	41.3	41.7	59.1	29.6	47.5
6027.06	4.08	-1.09	79.3	65.7	69.3	73.9	76.8	89.0	64.5	82.7
6056.01	4.73	-0.40	94.6	77.7	78.8	83.0	83.9	102.5	71.7	94.8
6079.01	4.65	-1.02	67.4	45.9	50.3	55.2	55.9	73.0	42.9	67.0
6089.57	5.02	-0.86	48.7	36.8	34.9	41.2	41.8	61.0	31.5	51.3
6151.62	2.18	-3.29	70.2	59.7	46.4	50.0	55.0	74.1	37.0	64.1
6157.74	4.07	-1.25	80.4	62.1	69.7	69.2	74.5	90.5	59.9	84.0
6159.38	4.61	-1.87	16.9	12.1	13.4	14.5	17.5	28.2	10.6	24.0
6165.37	4.14	-1.47	57.1	48.0	47.0	51.5	53.6	66.1	40.1	59.7
6180.21	2.73	-2.61	81.0	65.0	60.9	67.1	66.5	92.9	50.4	78.2
6187.99	3.94	-1.61	—	—	49.1	—	—	—	—	—
6200.32	2.61	-2.44	99.0	85.2	74.5	77.2	82.1	106.1	64.6	95.6
6226.74	3.88	-2.03	42.6	31.9	34.5	32.0	37.7	54.4	24.3	47.4
6229.23	2.84	-2.82	57.3	44.3	40.5	44.8	47.3	67.4	33.8	59.6
6240.65	2.22	-3.32	73.8	58.6	47.4	51.3	55.5	75.2	36.8	65.6
6265.14	2.18	-2.57	119.3	102.6	85.5	89.7	91.0	120.1	79.7	105.5
6270.22	2.86	-2.57	72.0	58.5	53.4	59.5	59.1	77.4	49.1	69.8
6380.75	4.19	-1.32	66.3	52.5	54.1	59.1	61.7	85.0	47.8	68.1
6392.54	2.28	-4.01	—	28.0	14.9	16.3	18.5	41.2	9.3	28.6
6498.95	0.96	-4.62	68.3	64.9	42.4	44.2	51.6	78.7	29.0	64.3
6591.33	4.59	-1.98	15.7	11.8	13.4	11.4	16.5	25.1	11.8	22.6
6608.04	2.28	-4.00	30.1	23.4	14.7	17.5	22.2	46.4	11.2	33.7
6627.56	4.55	-1.44	43.1	30.9	34.5	36.5	37.0	51.8	27.8	44.6
6646.93	2.61	-3.85	18.6	15.0	14.6	11.1	14.1	32.4	7.0	22.0
6653.91	4.15	-2.41	—	12.2	—	—	—	—	10.5	20.0
6703.58	2.76	-3.01	56.5	47.5	34.1	39.8	42.6	67.4	27.6	48.7
6710.31	1.48	-4.80	29.6	27.9	13.3	11.6	—	—	9.0	29.4
6725.36	4.10	-2.18	26.8	17.7	18.6	22.8	23.9	37.8	15.0	29.2
6726.67	4.61	-1.04	63.1	50.8	51.2	54.3	55.2	70.8	42.8	66.8
6733.15	4.64	-1.45	40.6	28.6	30.1	29.9	36.6	49.0	22.8	40.4
6745.11	4.58	-2.06	14.1	8.7	10.6	12.2	14.3	25.5	—	—
6750.15	2.42	-2.62	96.5	87.2	74.4	74.4	79.8	—	66.2	89.9
6752.72	4.64	-1.20	54.3	39.2	37.8	40.5	46.5	71.4	32.7	54.2
6786.87	4.19	-1.95	40.8	28.7	28.8	35.1	36.3	51.7	21.5	44.5
Fe II	$\log \epsilon_{\odot} = 7.47$									
5234.63	3.22	-2.20	88.5	60.8	106.9	106.9	99.4	94.2	114.9	94.2
6084.11	3.20	-3.75	17.7	8.6	35.5	37.5	30.9	28.9	39.8	28.9
6149.25	3.89	-2.70	33.2	16.2	57.7	55.5	51.0	41.0	61.0	41.0
6247.56	3.89	-2.30	55.7	25.1	80.4	83.9	72.5	52.1	88.5	52.1
6369.47	2.89	-4.11	19.0	6.5	31.8	34.2	30.7	22.4	36.9	22.4
6416.93	3.89	-2.60	43.6	24.4	56.5	55.8	53.2	49.1	62.5	49.1
6432.68	2.89	-3.29	39.1	18.8	58.8	63.6	53.1	46.6	66.0	46.6

Table 2. Line parameters and measured equivalent widths for C, O, S, Ca, Ti and Si lines.

λ_0	χ_i	$\log gf$	HD 1237	HD 13445	HD 52265	HD 75289	HD 82943	HD 83443	HD 169830	HD 202206
Equivalent Widths (mÅ)										
C I	$\log \epsilon_{\odot} = 8.56$									
5380.34	7.68	-1.71	17.0	7.8	39.4	39.0	36.3	26.1	45.1	22.5
6587.61	8.53	-1.08	9.9	—	29.6	27.8	24.9	—	36.2	16.7
O I	$\log \epsilon_{\odot} = 8.93$									
6300.30	0.00	-9.84	—	—	5.1	3.2	5.2	9.7	—	—
S I	$\log \epsilon_{\odot} = 7.21$									
6046.03	7.87	-0.23	15.1	—	27.3	28.3	29.0	25.4	31.6	18.0
6052.67	7.87	-0.44	8.8	—	24.1	21.2	20.1	18.7	26.0	14.3
Ca I	$\log \epsilon_{\odot} = 6.36$									
5867.57	2.93	-1.56	40.8	36.3	25.5	31.6	29.4	49.2	17.6	40.4
6166.44	2.52	-1.10	90.3	91.1	72.1	75.4	76.9	101.1	61.0	89.2
6169.05	2.52	-0.68	137.9	128.1	97.5	102.0	101.1	138.7	86.9	116.4
6455.62	2.52	-1.34	77.4	69.4	61.9	62.2	64.9	88.5	52.8	75.0
6471.66	2.53	-0.80	123.0	118.5	112.7	101.5	108.4	127.9	87.7	110.0
6499.65	2.52	-0.90	114.9	106.2	88.8	93.1	95.4	118.1	82.7	108.9
6508.81	2.53	-2.33	32.6	16.3	7.4	14.9	14.4	26.8	6.2	24.5
Ti I	$\log \epsilon_{\odot} = 4.99$									
5087.06	1.43	-0.88	53.1	69.8	25.2	31.3	33.1	78.1	18.0	48.0
5113.45	1.44	-0.91	48.2	65.0	24.7	27.5	30.5	60.1	15.3	44.1
5300.01	1.05	-1.47	28.4	28.1	—	—	—	52.0	17.5	—
5426.25	0.02	-3.05	18.1	26.2	—	—	8.2	33.2	3.0	12.1
5866.46	1.07	-0.92	72.3	83.3	46.3	48.8	51.3	91.4	30.1	65.1
5965.84	1.88	-0.38	53.2	55.1	36.0	30.7	45.4	80.3	21.7	46.3
6126.22	1.07	-1.41	43.0	48.0	18.2	19.5	24.0	55.0	13.0	43.0
6261.11	1.43	-0.46	74.1	81.4	46.2	49.2	53.1	94.8	32.9	70.2
Ti II	$\log \epsilon_{\odot} = 4.99$									
4589.96	1.23	-1.61	89.2	74.6	101.4	105.3	98.1	101.3	106.9	94.8
5336.78	1.58	-1.61	73.2	60.1	88.0	89.5	81.8	85.0	94.1	77.0
5418.77	1.58	-2.07	52.1	37.0	61.4	64.1	60.2	61.2	67.1	57.1
Si I	$\log \epsilon_{\odot} = 7.55$									
5665.56	4.92	-1.98	51.0	34.3	50.6	50.7	53.1	—	40.3	61.6
5690.43	4.93	-1.82	59.5	41.9	56.9	61.4	62.1	72.7	52.5	65.6
5793.07	4.93	-1.96	52.2	36.3	55.7	57.6	59.0	73.2	50.7	61.7
5948.54	5.08	-1.08	101.1	87.8	105.7	97.5	118.5	131.7	86.7	109.0
6091.91	5.87	-1.36	48.1	26.6	53.1	55.0	58.9	89.2	40.8	—
6125.01	5.61	-1.51	39.9	26.9	45.5	45.2	50.7	57.4	37.2	53.4
6142.47	5.62	-1.48	35.3	25.7	46.0	49.5	52.9	61.8	38.4	51.9
6155.15	5.62	-0.72	97.2	66.2	105.6	107.2	118.1	131.3	90.5	114.6
6237.34	5.61	-1.06	78.6	48.2	85.9	88.6	90.2	116.0	71.4	94.0
6583.69	5.95	-1.65	18.9	14.7	34.2	37.5	34.3	44.6	21.4	40.7
6721.86	5.86	-1.14	53.7	34.1	60.6	63.9	65.7	85.2	50.2	73.5

Table 5. Final $[X/H]$ values.

ele.	HD 1237	HD 13445	HD 52265	HD 75289	HD 82943	HD 83443	HD 169830	HD 202206
C	+0.01±0.14	+0.08±0.11	+0.18±0.10	+0.15±0.13	+0.22±0.13	+0.40±0.11	+0.10±0.09	+0.17±0.10
O	–	–	+0.07±0.09	−0.02±0.09	+0.25±0.09	+0.50±0.09	–	–
S	+0.15±0.10	–	+0.13±0.10	+0.09±0.06	+0.20±0.05	+0.46±0.06	+0.04±0.07	+0.15±0.10
Ca	+0.10±0.13	−0.23±0.11	+0.19±0.19	+0.24±0.06	+0.24±0.10	+0.24±0.10	+0.15±0.12	+0.25±0.08
Ti I	+0.11±0.12	−0.01±0.25	+0.22±0.08	+0.31±0.08	+0.34±0.08	+0.49±0.18	+0.22±0.11	+0.34±0.10
Ti II	+0.02±0.09	−0.16±0.07	+0.23±0.13	+0.29±0.11	+0.38±0.12	+0.43±0.13	+0.28±0.14	+0.41±0.12
Si	+0.13±0.07	−0.09±0.09	+0.32±0.08	+0.33±0.10	+0.39±0.06	+0.57±0.12	+0.23±0.06	+0.40±0.09

**Fig. 2.** Fe I abundances for HD 169830 computed using the atmospheric parameters from Table 3. The dashed lines represent the fit to the points. *Upper panel:* abundance vs. reduced equivalent width; *lower panel:* abundance vs. lower excitation potential.

3.3. Comparison with former results

Previous spectroscopic analysis have been reported by different authors only for three stars from the present sample.

A value of $[Fe/H] = -0.24$ was determined by Flynn & Morell (1997) for HD 13445. Our value of -0.21 , as well as all the atmospheric parameters are in good agreement with those proposed by these authors. The small differences can be understood if we note that these authors used different models of atmospheres and a small number of Fe lines.

The comparison of our atmospheric parameters with those of Gonzalez & Laws (2000) for HD 75289 shows that they are remarkably similar. This similarity comes probably from the fact that we used the same line-list, models

Table 3. Stellar parameters determined from the Fe lines.

HD number	T_{eff} (K)	$\log g$ (cm s^{-2})	ξ_t (km s^{-1})	$[Fe/H]$
1237	5540±75	4.70±0.20	1.47±0.1	+0.10±0.08
13445	5180±75	4.75±0.25	0.79±0.1	−0.21±0.07
52265	6060±50	4.29±0.25	1.29±0.1	+0.21±0.06
75289	6140±50	4.47±0.20	1.47±0.1	+0.28±0.07
82943	6010±50	4.62±0.20	1.08±0.1	+0.32±0.06
83443	5460±100	4.55±0.25	1.05±0.1	+0.38±0.11
169830	6300±50	4.11±0.25	1.37±0.1	+0.21±0.05
202206	5750±75	4.80±0.20	0.96±0.1	+0.36±0.08

Table 4. Sensitivities of $[X/H]$ values due to changes in T_{eff} of +100 k, and $\log g$ of +0.2 dex for HD 13445 and HD 169830.

Star/Element	$\Delta T_{\text{eff}} = +100 \text{ k}$	$\Delta \log g = +0.2 \text{ dex}$
HD 13445		
C	−0.08	+0.08
Ca	+0.09	−0.06
Ti I	+0.12	−0.03
Ti II	0.00	+0.06
Si	−0.02	+0.02
Fe	+0.05	+0.01
HD 169830		
C	−0.06	+0.07
S	−0.04	+0.04
Ca	+0.06	−0.02
Ti I	+0.08	−0.01
Ti II	+0.02	+0.07
Si	+0.04	−0.01
Fe	+0.07	0.00

of atmospheres and the spectrum synthesis tool (MOOG). It is also apparent that the use of a different spectrograph/configuration does not have a significant influence on the final results (e.g. $[Fe/H]$ and other abundance ratios). The difference is large only for Ca (more than 0.05

dex). In this paper we add the results for oxygen, not determined by these authors.

HD 169830 was included in the large survey of Edvardsson et al. (1993). They obtained $T_{\text{eff}} = 6382$ K, $\log g = 4.15$ and $[\text{Fe}/\text{H}] = +0.13$. These values are perfectly compatible with our results, even though they used a rather different iron line list and a different model atmosphere. The value for $[\text{Fe}/\text{H}]$ is slightly lower than ours, which may be partially explained by the fact that they adopted the meteoritic value of $\log \epsilon_{\odot}(\text{Fe})$ of 7.51.

Gustafsson et al. (1999) provided carbon abundance for this star using the $[\text{C I}]$ line at 8727.14 \AA . Taking the stellar parameters determined by Edvardsson et al. (1993), they find $[\text{C}/\text{H}] = +0.19$, 0.09 dex higher than our estimate. Below we will discuss carbon abundances in more detail.

4. Discussion

4.1. Metallicity-giant planet connection

As we can see from tables 3 and 5, the planetary host star candidates studied in this work have abundances above Solar for almost all elements, the only exception being HD 13445.

It is interesting to notice that 3 of the objects are Super Metal Rich (SMR) candidates (defined as having $[\text{Fe}/\text{H}] > 0.2$ with 95% confidence, Taylor 1996), namely HD 82943, HD 83443 and HD 202206. HD 83443 has the planet in the closest orbit detected to date (only 0.028 A.U.), and one of the least massive companions (1.17 times the mass of Saturn). This seems to confirm that even the lowest mass companions orbit metal-rich stars.

In Fig. 3 we compare the distribution of the $[\text{Fe}/\text{H}]$ values for stars with planets with the $[\text{Fe}/\text{H}]$ distribution of a volume-limited sample of field stars (here we used the original distribution of Favata et al. (1997), not corrected for scale galactic height effects). This kind of plot was first done by Gonzalez et al. (1998) and later revisited by Butler et al. (2000). However, the addition of 6 new planets and 2 brown dwarfs clearly deserves a revision.

The values of $[\text{Fe}/\text{H}]$ for stars with planets were taken from Table 3 and, for the stars not included in this paper, from different authors and compiled in Table 4 of Butler et al. (2000). We did not include the known Brown Dwarf candidates (HD 114762, HD 162020, and HD 202206) in the histogram, but their position in the diagram is represented by the vertical lines. For HD 108147, HD 162020, and HD 168746 we found no spectroscopic values of $[\text{Fe}/\text{H}]$ in the literature, and we thus determined $[\text{Fe}/\text{H}]$ from the *ubvy*-photometry of Hauck & Mermilliod (1997), and using the calibration of Schuster & Nissen (1989); we obtained $[\text{Fe}/\text{H}] = -0.02$, 0.11, and -0.09 , respectively. For HD 114762 we took the spectroscopic value of $[\text{Fe}/\text{H}] = -0.60$ obtained by Gonzalez (1998).

As we can see from Fig. 3, the addition of the 6 new planets to the histogram further supports the former ideas

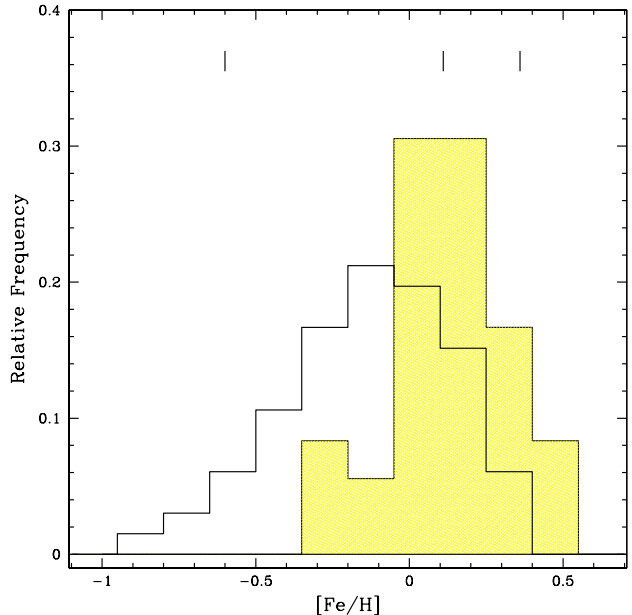


Fig. 3. Metallicity distribution of stars with planets (shaded histogram) compared with the same distribution for field G and K dwarfs (Favata et al. 1997). The vertical lines represent stars with brown dwarf candidate companions.

that stars with planets are particularly metal rich when compared with field solar-type dwarfs. This result cannot be related to a selection bias, since the most important planet search programmes make use of volume limited samples of stars (Udry et al. 2000; Marcy et al. 2000). The only exception is BD-103166 (Butler et al. 2000), chosen for its high metallicity. The simple fact that of the 6 new planets announced by the Geneva group, 5 were discovered around metal-rich dwarfs, clearly shows that the trend is certainly real.

The position of the three Brown Dwarf candidates (HD 114762, HD 162020, and HD 202206), is intriguing and interesting. Two of the candidates have metallicities that place them perfectly inside the “planetary” metallicity distribution. This is particularly evident for HD 202206 for which we find $[\text{Fe}/\text{H}] = +0.36$. If the metallicity of the stars with planets is in fact related to their formation process, this fact suggests that the frontier between brown dwarfs and extra-solar giant planets is not very well defined, and there may be some overlapping. But this can also probably be explained if we consider that HD 202206 is in the metal-rich tail of the field distribution. The inclusion of more brown dwarfs into this plot is essential to better clarify this situation.

It is important to refer, however, that we are comparing two distributions whose chemical analysis were performed using two different methods. In the present article, effective temperatures were derived from Fe lines

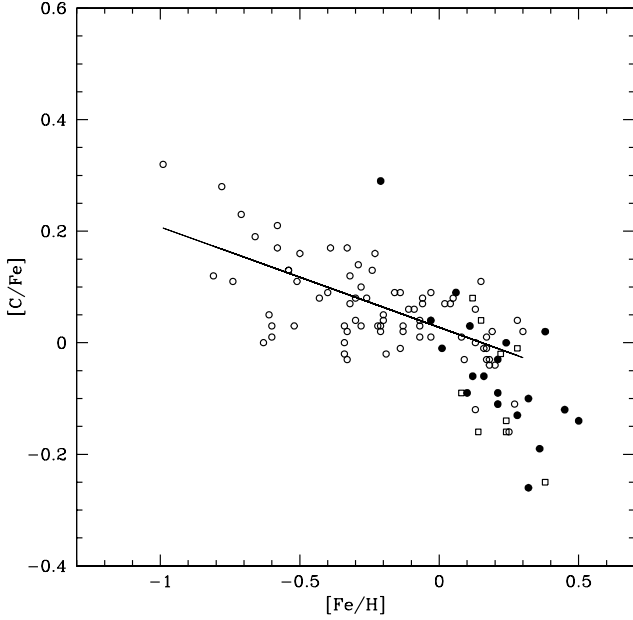


Fig. 4. Plot of $[C/H]$ vs. $[Fe/H]$ for stars with planets (filled circles) and for field stars, included in the studies of Gustafsson et al. (1999) and Tomkin et al. (1997), the open circles and open squares, respectively. The line represents the best linear fit to the distribution of Gustafsson et al.

formed in LTE, while Favata et al. (1997) derived them from colours. We do not think that this may account for the observed differences in the $[Fe/H]$ distributions. However, we cannot exclude that the use of a uniform analysis may lead to somewhat different results.

4.2. Elements other than Fe

Gonzalez & Laws (2000) suggested that stars with planetary companions might be carbon deficient when compared with field dwarfs. In Fig. 4 we compare the distribution of $[C/Fe]$ for stars with planets (filled circles) to the results obtained in the survey of 80 late-F and early-G dwarfs of Gustafsson et al. (1999), and of the work of Tomkin et al. (1997).

Although we have the impression that stars with planets are located below the trend for field stars, we believe that statistically we cannot make any serious conclusion. If we take only the distribution of Gustafsson et al., we would have the impression that stars with planets are positioned below the main trend. However, the addition of the study of Tomkin et al. adds a few points to the region where stars with planets are located.

It is important to mention that all “three” studies were done using different sets of lines. Gustafsson et al. used the 8727Å line, while the study of Tomkin et al. made use of 6 different carbon lines. Furthermore, the values for the stars with planets are a compilation of the results of this

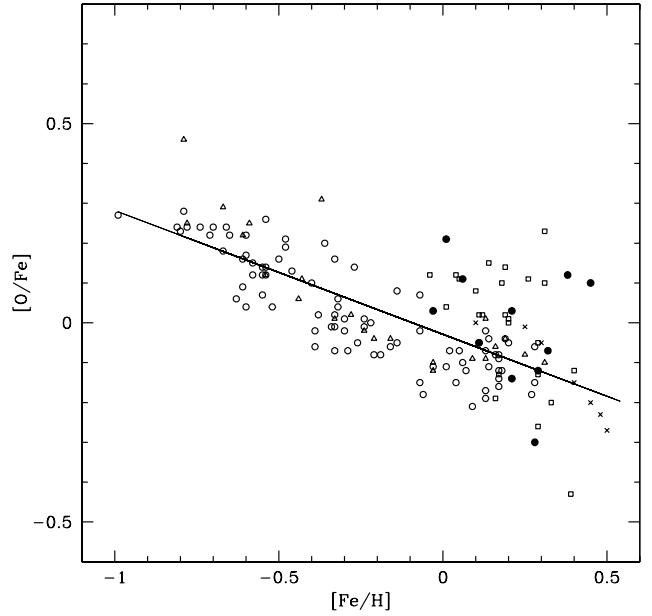


Fig. 5. Plot of $[O/Fe]$ vs. $[Fe/H]$ for stars with planets (filled circles) when compared with the study of field dwarfs of Feltzing & Gustafsson (1998), open squares, Edvardsson et al. (1993), open circles, Castro et al. (1997), crosses, and Nissen & Edvardsson (1992), open triangles. Values for stars with planets were taken from this paper and from Gonzalez & Vanture (1998), Gonzalez (1998), and Sadakane et al. (1999). The best linear fit to the field star data is also presented.

paper and of Gonzalez & Laws (2000), Gonzalez (1998), and Sadakane et al. (1999). The slight trend that we see, favoring the position of stars with planets in the low part of the mean trend line may thus be the result of systematics in the determination of carbon abundances, connected with the use of different lines and maybe of different atmosphere models (MARCS vs. ATLAS). Given that all stars with planets are positioned at the right limit of the plot ($[Fe/H]$ rich stars), we cannot completely exclude the existence of a change in the slope of the relation $[C/Fe]$ vs. $[Fe/H]$ for very metal-rich dwarfs, connected or not with the presence of planets.

Given all these points, we prefer to be cautious concerning this result. The resolution of this problem may need a consistent and uniform study of carbon abundances in metal rich dwarfs, using the same set of lines and atmosphere models.

Oxygen and other α -elements are produced in massive stars exploding as Type II supernovae. Many studies of the Galactic disk stars support a view that $[O/Fe]$ declines from $[O/Fe] \sim 0.5$ at $[Fe/H] = -1$ to about 0 at $[Fe/H] = 0$ (Chen et al. 2000; Edvardsson et al. 1993; Feltzing & Gustafsson 1998). It is commonly accepted that this decline is due to the enhanced contribution of iron

from Type Ia supernovae at about $[\text{Fe}/\text{H}] = -1$. Similar trends (but not as steep as for oxygen) were found for other α -elements. It was also found that the differences in $[\alpha/\text{Fe}]$ in the metallicity range $-0.8 < [\text{Fe}/\text{H}] < -0.4$ are correlated with the mean orbital galactocentric distance. Namely, stars with large Galactic orbits (exceeding 9 kpc), have $[\alpha/\text{Fe}]$ smaller than stars in the inner orbits.

The situation is more complicated at metallicities $[\text{Fe}/\text{H}] > -0.1$. Galactic viscous disk models of Tsujimoto et al. (1995) predict $[\text{O}/\text{Fe}]$ vs. $[\text{Fe}/\text{H}]$ to flatten out at solar metallicities. However, observations of Feltzing & Gustafsson (1998) show that the $[\text{O}/\text{Fe}]$ decline continues even at $[\text{Fe}/\text{H}] > 0$. It is interesting to plot stars with planets on the same $[\text{O}/\text{Fe}]$ vs $[\text{Fe}/\text{H}]$ graph together with the field metal rich stars in order to find out whether or not our targets follow the Galactic trend discussed by Feltzing & Gustafsson. Combining the $[\text{O}/\text{Fe}]$ ratios reported in this paper together with the values presented in the literature we found a large scatter on the $[\text{O}/\text{Fe}]$ vs $[\text{Fe}/\text{H}]$ diagram (Fig. 5) for stars with $[\text{Fe}/\text{H}] > 0$. It is interesting that HD 75289 and HD 82943 have very similar abundances of all elements except oxygen which provides $[\text{O}/\text{Fe}] = -0.30$ and -0.07 , respectively. Another interesting case was observed in HD 217107 where α -elements Mg, Si and S are enhanced with respect to $[\text{Fe}/\text{H}]$ by about 0.2 dex while oxygen is again under-abundant (Sadakane et al. 1999). Note that for HD 83443 we derived $[\text{O}/\text{Fe}] = 0.12$. The small number of observations and a use of only one oxygen line prevents us making from any firm conclusions. It would help to study different oxygen lines (IR triplets at 7775 and 8446 Å, OH bands in the near-UV and IR) in order to obtain consistent abundances from the lines formed in different atmospheric layers.

In Fig. 6 we present the plots for $[\text{X}/\text{Fe}]$ as a function of $[\text{Fe}/\text{H}]$ for $\text{X} = \text{Ca}$, Ti , and Si , as compared with the values obtained by Feltzing & Gustafsson (1998) in their survey of 47 G and K dwarfs. The values of $[\text{X}/\text{H}]$ for the stars with planets were taken from this paper and from Gonzalez & Laws (2000), Gonzalez (1998), and Sadakane et al. (1999).

An analysis of the figure shows that there are no apparent trends distinguishing stars with planets from single stars. This result does not exclude that stars with planets may have a different “behavior” in such plots, but it definitely shows that if they exist, then they must be of the order of 0.1 dex or lower (considering the errors in the determinations of the abundances).

Moreover, comparison of Ca and Ti abundances in the stars with planets with those from the field (Edvardsson et al. 1993; Feltzing & Gustafsson 1998) confirms previous findings that $[\text{Ca}/\text{Fe}]$ and $[\text{Ti}/\text{Fe}]$ flattens out towards higher metallicities. We confirm a small scatter in $[\text{Ca}/\text{Fe}]$ and $[\text{Ti}/\text{Fe}]$ found by these authors. Our data for Si does not show a large scatter as found by Feltzing & Gustafsson (1998). Observations of Chen et al. (2000) support the small scatter found for Si in our study.

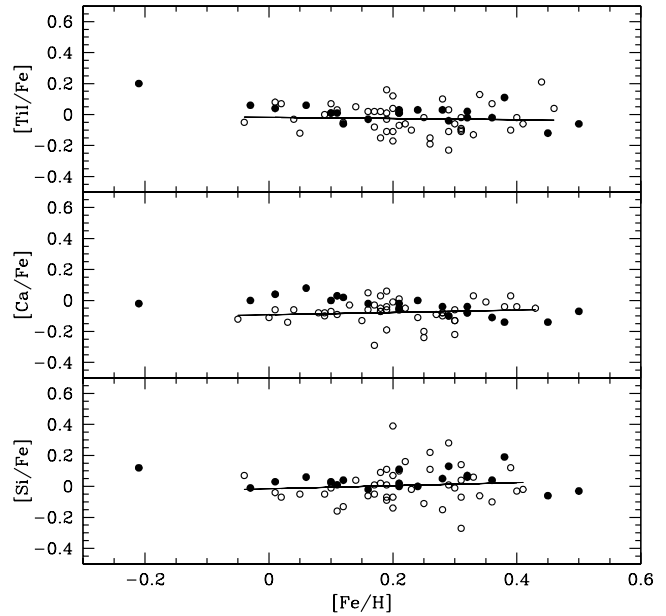


Fig. 6. Plots of $[\text{X}/\text{Fe}]$ vs. $[\text{Fe}/\text{H}]$ for three α -elements. Open circles represent field stars from the study of Feltzing & Gustafsson (1998), and filled circles stars with planetary mass companions. Fits to the field star sample are also shown.

4.3. Primordial abundance vs. Enrichment

Various formation models try to take into account the observed anomalies to explain how and why the observed systems were formed and evolved. In the continuation of the conventional picture where an “ice” core is needed to accrete gas and give origin to a giant planet, the “new” theories include inward migration of the formed planet due to gravitational interaction with the disk (Goldreich & Tremaine 1980; Lin & Papaloizou 1986; Lissauer 1995), gravitational interactions between multiple giant planets (Weidenschilling & Marzari 1996; Rasio & Ford 1996) or even *in-situ* formation (e.g., Wuchterl 1996; Bodenheimer et al. 1999), which was not compatible with former theories of giant gaseous planet formation. In these scenarios, the explanation of the higher metallicity found in giant extra-solar planet mother stars may involve mechanisms like the transfer of material from the disk to the star as the result of the migration processes (Lin & Papaloizou 1986), or the fall of one or more planets into the star. On the other hand, these anomalies can also be “explained” if we invoke that the formation of giant planets is dependent on the metallicity of the original molecular cloud.

Since the mass of the convective envelope of a solar type dwarf increases with increasing spectral type, if the enrichment scenario is the key of the observed chemical anomalies, we might expect that the value of $[\text{Fe}/\text{H}]$ would be anti-correlated with the mass of the convective enve-

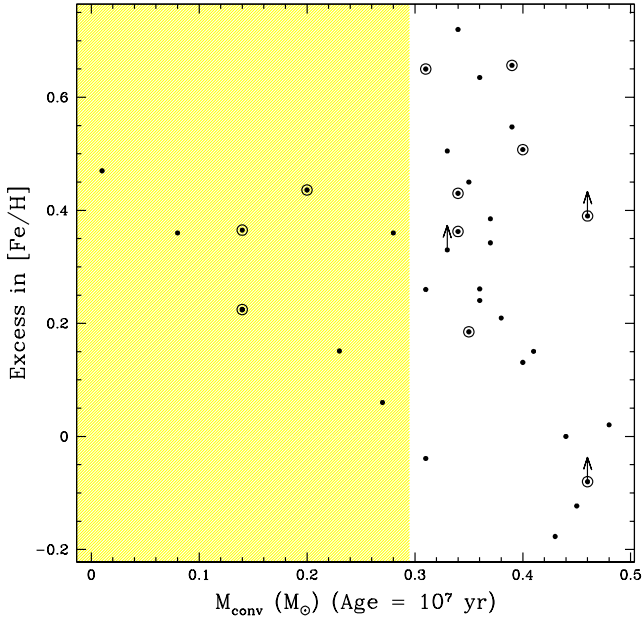


Fig. 7. Plot of the mass of the convective envelope as a function of $[\text{Fe}/\text{H}]$. “Solar” symbols denote stars with planets orbiting closer than ~ 0.08 AU. The shaded region represents the part of the diagram for which we believe there are observational biases. Arrows represent objects for which no age was estimated, and an age of 0.0 yrs was considered.

lope at the time of planetary formation. This is particularly true for stars with planets in close orbits, since the migration process is expected to induce the fall of H and He poor disk material that was inside the orbit of the planet (Lin et al. 1996).

To test this hypothesis we plot in Fig. 7 the values of the $[\text{Fe}/\text{H}]$ excess for the extra-solar planet harboring stars listed in Table 6, against the mass of the convection zone (M_{conv}). The $[\text{Fe}/\text{H}]$ excess is defined here as being the difference between the observed value and the one expected according to the relation obtained by Gonzalez (1999):

$$[\text{Fe}/\text{H}] = -0.035 \text{ Age}(\text{Gyr}) - 0.01 \quad (1)$$

This correction is done in order to take into account the galactic age gradient; it did not, however, change particularly the distribution of the stars in the diagram. We do not make any correction for galactocentric distance. This does not, in principle, introduce any systematic errors.

The ages were taken from different authors (see Table 6), and when no values were available, they were computed from the Ca II emission measure R'_{HK} using the relation of Donahue (1993), also quoted in Henry et al. (1996). For three of the objects we have no value for the age: because of their position in the H-R diagram the errors computed using evolutionary tracks are very high; no R'_{HK} was available for these objects.

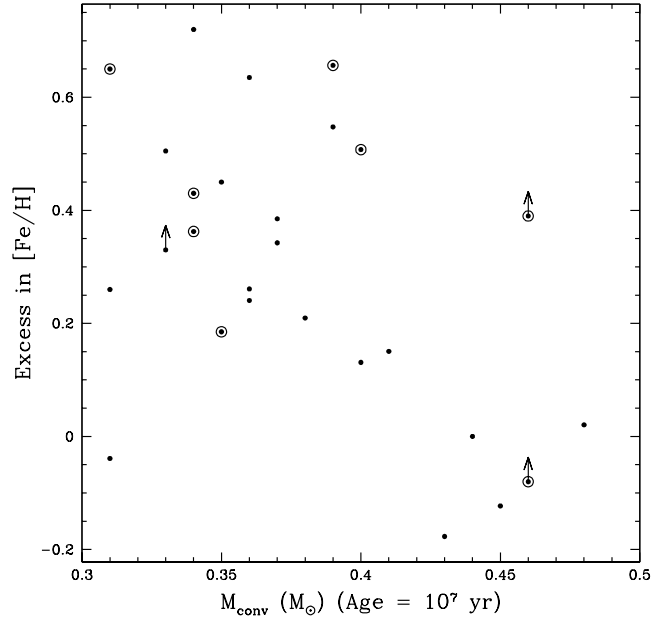


Fig. 8. Same as in Fig 7 but for the region with $M_{\text{conv}} \geq 0.3 M_{\odot}$.

The masses for the convective envelopes (M_{conv}) were derived from Table 1 of D’Antona & Mazzitelli (1994), considering an age of 10^7 yr, and the stellar masses published by Butler et al. (2000). For the stars not listed by these authors, stellar masses were derived from the position of the star in the evolutionary tracks of Schaller et al. (1992). The age of 10^7 Gyr was taken to be the life time of a proto-planetary disk (Zuckerman et al. 1995), and thus a probable value for disk contamination to occur.

One interesting feature to note in the plot is that the region with $M_{\text{conv}} \leq 0.3 M_{\odot}$ (shaded region) has a very low number of stars. But rather than having a physical origin, we believe that the reason for this effect has to do with sampling effects. The stars in this region are late-F and early-G dwarfs. Dwarfs of these spectral types are usually fast rotators, consequently having higher intrinsic radial-velocity “jitter” (Mayor et al. 1998; Saar et al. 1998; Santos et al. 2000), and thus more difficult targets for high-precision radial-velocity searches for planets. Also, given their masses, a random sample of F dwarfs must be in general younger and thus more metal-rich than an equivalent sample of G dwarfs. This may explain the fact that stars in this region are slightly above the mean $[\text{Fe}/\text{H}]$ in the plot. Given these biases, we will concentrate on the right side of the diagram, plotted in more detail in Fig 8.

This plot gives the impression that some trend exists in the sense of an anti-correlation. This is due to the presence of a very few stars in the lower-right corner of the diagram. However, a linear fit to the points shows no significant correlation (we obtain a Spearman correlation coefficient of -0.3).

Table 6. Values used to make the plots of Figures 7, 8, and 9. For the references, G99, F99, and M00 correspond to Gonzalez (1999), Fischer et al. (1999), and Mazeh et al. (2000), respectively.

Star	[Fe/H] observed	Age (Gyr)	Age Reference	[Fe/H] from age	[Fe/H] excess	M_{star} (M_{\odot})	M_c (10^7 yr) (M_{\odot})	M_c (10^8 yr) (M_{\odot})
BD −10 3166	0.50	4	Ca II	-0.15	0.65	1.10	0.31	0.012
HD 1237	0.10	0.6	Ca II	-0.03	0.13	0.96	0.40	0.037
HD 9826	0.12	2.7	G99	-0.10	0.22	1.30	0.14	0.000
HD 12661	0.32	—	—	-0.01	0.33	1.07	0.33	0.019
HD 13445	-0.21	2.2	Ca II	-0.09	-0.12	0.86	0.45	0.050
HD 16141	0.02	6.6	Ca II	-0.24	0.26	1.03	0.36	0.024
HD 17051	0.11	0.9	Ca II	-0.04	0.15	1.19	0.23	0.000
HD 37124	-0.32	3.8	Ca II	-0.14	-0.18	0.91	0.43	0.046
HD 46375	0.34	4.5	Ca II	-0.17	0.51	0.96	0.40	0.037
HD 52265	0.21	4	Ca II	-0.15	0.36	1.13	0.28	0.007
HD 75289	0.23	5.6	Ca II	-0.21	0.44	1.22	0.20	0.000
HD 75732	0.45	5.0	G99	-0.19	0.64	1.03	0.36	0.023
HD 82943	0.32	5	Ca II	-0.19	0.51	1.08	0.40	0.015
HD 83443	0.38	—	—	-0.01	0.39	0.85	0.46	0.051
HD 89744	0.18	8	Ca II	-0.29	0.47	1.43	0.01	0.000
HD 95128	0.01	6.3	G99	-0.23	0.24	1.03	0.36	0.023
HD 108147	-0.02	2	Ca II	-0.08	0.06	1.15	0.31	0.005
HD 117176	-0.03	8	G99	-0.29	0.26	1.10	0.31	0.012
HD 120136	0.32	1	G99	-0.05	0.37	1.30	0.14	0.000
HD 130322	-0.02	0.3	Ca II	-0.02	-0.00	0.89	0.44	0.050
HD 134987	0.23	6.0	Ca II	-0.22	0.45	1.05	0.35	0.021
HD 143761	-0.29	12.3	G99	-0.44	0.15	0.95	0.41	0.039
HD 145675	0.50	6	G99	-0.22	0.72	1.06	0.34	0.019
HD 168443	-0.14	2.6	Ca II	-0.10	-0.04	1.10	0.31	0.012
HD 168746	-0.09	—	—	-0.01	-0.08	0.86	0.41	0.051
HD 169830	0.21	4	Ca II	-0.15	0.36	1.37	0.04	0.000
HD 186427	0.06	9	G99	-0.33	0.39	1.01	0.37	0.027
HD 187123	0.16	5.5	G99	-0.20	0.36	1.06	0.34	0.019
HD 192263	0.00	0.3	Ca II	-0.02	0.02	0.79	0.48	0.062
HD 195019	0.00	9.5	F99	-0.34	0.34	1.02	0.37	0.026
HD 209458	0.00	5	M00	-0.19	0.19	1.05	0.35	0.021
HD 210277	0.24	8.5	G99	-0.31	0.55	0.99	0.39	0.031
HD 217014	0.21	6	G99	-0.22	0.43	1.06	0.34	0.019
HD 217107	0.30	9.9	F99	-0.36	0.66	0.98	0.39	0.033
HD 222582	0.00	5.7	Ca II	-0.21	0.21	1.00	0.38	0.029

It is important at this point to discuss the sources of uncertainties in the diagram. First of all, the mass of the convection zone changes very fast with age in those evolutionary ages. For a $1 M_{\odot}$ star, if instead of 10^7 we take $3 \cdot 10^7$ yr, the difference in the mass of the convection zone increases by about $0.3 M_{\odot}$. It is possible that disk contamination can happen in slightly different time scales for different stars, and thus the final result would be completely different. Furthermore, the contamination scenario itself is not simple. If instead of disk contamination we imagine that one or more planets fell into the star (by dynamical interactions in a multiple system), this would not necessarily take place at the same time in a star’s life. And of course, why should one expect that all stars would be “polluted” by the same amount of material? These facts may

probably explain, or at least contribute, to the observed dispersion.

Adding to these errors, the precision of eqn. 1 is difficult to establish, but errors of the order of 0.2 to 0.3 dex are expected. The errors in the age are also not measurable, but might amount to some Gyr. To these we must add the uncertainties in the stellar models.

On the other hand, the analysis of the plot of Fig. 8 poses another problem: how can we explain that “contamination” effects may have increased the $[Fe/H]$ by more than 0.6 dex in stars with convection envelopes having masses around $0.35 M_{\odot}$? For example, the fall of 10 earth masses of iron into a star with a convective envelope having solar metallicity and a mass of $0.3 M_{\odot}$ would increase the $[Fe/H]$ by an insignificant amount. If the abundances

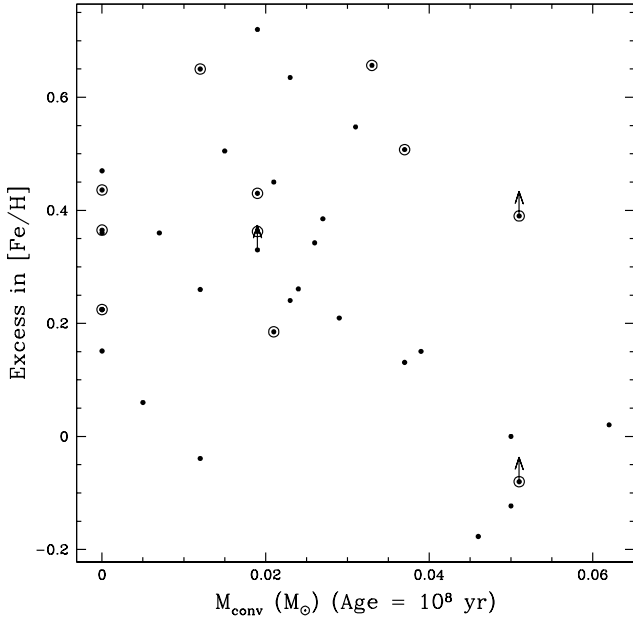


Fig. 9. Same as in Fig 7 but for M_{conv} values at age = 10^8 yr.

are really due to some enrichment process, then they must probably have taken place much after 10^7 yr. If the disk time-scales are correct, this would imply that the process did not involve the fall of disk material, but the addition of formed planets.

In Fig. 9 we have thus made a plot of the same variables, but this time M_{conv} was computed for an age of 10^8 yr. Still no correlation is evident. Although the size of the convection envelope has dropped, it seems unlikely that the high values observed for the $[Fe/H]$ excess can be explained in an enrichment scenario (due to the fall of one or multiple planets). The convective outer envelope of the Sun at an age of 10^8 yr represents about 3% of the total mass, and the fall of the same quantity of iron would change the abundance by about ~ 0.15 dex. This value would drop if we take a giant gaseous planet, containing a certain amount of H and He. To have an excess of $[Fe/H]$ of the order of 0.6 dex we have to imagine that a star like the Sun had to swallow about 30 earth masses of iron. Considering the composition of C1 chondrites, this would mean ~ 5 times more in silicate material, a value that seems excessively high. Unless multiple silicate-rich giant planets fell into the star, this result clearly supports the idea that the cause of the excess of iron is probably “primordial”. Since the high $[Fe/H]$ vs. existence of planet relation is not in cause, these arguments favor a scenario where the formation of giant planets is dependent on the metallicity of the parent cloud.

5. Concluding remarks

We have presented an abundance analysis of 7 stars known to harbor giant planets and one with a brown dwarf candidate. The results obtained further support the idea that stars with planets are metal rich when compared with field dwarfs.

We discuss two possible scenarios that could explain the observed anomalies. The results are still not conclusive, but support the idea that a star needs to be formed out of a metal-rich cloud to form giant planets.

One other important conclusion comes out of the present work: to be able to search and study hypothetical chemical anomalies in elements other than iron one must lower the errors in the abundance determination to at least 0.1 dex. This should be possible in the context of a high resolution and S/N spectroscopic study, using for all objects the same spectral lines, atmosphere models, and if possible making use of a comparison set of stars without planetary companions and with similar atmospheric parameters.

Acknowledgements. We wish to thank the Swiss National Science Foundation (FNSRS) for the continuous support to this project. We would also like to thank Claudio Melo, Daniel Ersparmer, Pierre North, André Maeder and Bernard Pernier for useful discussions. Support from Fundação para a Ciência e Tecnologia, Portugal, to N.C.S. in the form of a scholarship is gratefully acknowledged.

References

- Anders E., Grevesse N., 1989, *Geochim. et Cosmochim. Acta* 53, 197
- Bodenheimer P., Hubickyj O., Lissauer J.J., 1999. In: “Protostars, & Planets IV”, Mannings V., Boss A., Russel S. (eds.), University of Arizona Press, Tucson, in press
- Butler R.P., Vogt S.S., Marcy G.W., et al., 2000, *ApJ* submitted
- Castro S., Michael Rich R., Grenon M., et al., 1997, *AJ* 114, 376
- Chen Y.Q., Nissen P.E., Zhao G., Zhang H.W., Benoni T., 2000, *A&AS* 141, 491
- D’Antona F., Mazzitelli I., 1994, *ApJS* 90, 467
- Donahue R.A., 1993, PhD Thesis, New Mexico State University
- Edvardsson B., Andersen J., Gustafsson B., et al., 1993, *A&A* 275, 101
- Favata F., Micela G., Sciortino S., 1997, *A&A* 323, 809
- Feltzing S., Gustafsson B., 1998, *A&AS* 129, 237
- Fischer D., Marcy G.W., Butler R.P., et al., 1999, *PASP* 111, 50
- Flynn C., Morell O., 1997, *MNRAS* 286, 617
- Goldreich P., Tremaine S., 1980, *ApJ* 241, 425
- Gonzalez G., 1997, *MNRAS* 285, 403
- Gonzalez G., 1998, *A&A* 334, 221
- Gonzalez G., 1999, *MNRAS* 308, 447
- Gonzalez G., Laws C., 2000, *AJ* 119, 390
- Gonzalez G., Vanture A.D., 1998, *A&A* 339, L29

- Gustafsson B., Harlsson T., Olsson, E., Edvardsson B, Ryde N., 1999, A&A 342, 426
- Hauck B., Mermilliod M., 1997, A&AS 129, 431
- Henry T.J., Soderblom D.R., Donahue R.A., Baliunas S.L., 1996, AJ 111, 439
- Kurucz R. L., 1993, CD-ROMs, ATLAS9 Stellar Atmospheres Programs and 2 km s⁻¹ Grid (Cambridge: Smithsonian Astrophys. Obs.)
- Kurucz R. L., Furenlid, I., Brault, J., Testerman, L. 1984, Solar Flux Atlas from 296 to 1300 nm, NAOA Atlas No. 1
- Lin D., Bodenheimer P., Richardson D.C., 1996, Nat 380, 606
- Lin D., Papaloizou J., 1986, ApJ 309, 846
- Lissauer J., 1995, Icarus 114, 217
- Marcy G.W., Cochran W.D., Mayor M., 1999. In: "Protostars, & Planets IV", Mannings V., Boss A., Russel S. (eds.), University of Arizona Press, Tucson, in press
- Marcy G.W., Butler R.P., Vogt S., 2000, ApJ 536, L43
- Mayor M., Queloz D., 1995, Nat 378, 355
- Mayor M., Queloz D., Udry S., 1998. In: Baliunas S., Ambruster C., Garmany C., Giampapa M.S., Janes K. (eds.) Proc. of the conference "Brown dwarfs and extra-solar planets", A.S.P. Conference Series Publications 134
- Mazeh M., Naef, D., Torres G., et al., 2000, ApJ 532, L55
- Naef D., Mayor P., Pepe F., et al., 2000. In: Gárzon F., Eiroa C., de Winter D., Mahoney T.J. (eds.) Proc. of the conference "Disks, Planetesimals and Planets", A.S.P. Conference Series, in press
- Nissen P.E., Edvardsson B., 1992, A&A 261, 255
- Olsen E.H., 1984, A&AS 57, 443
- Queloz D., Mayor M., Weber L., et al., 2000, A&A 354, 99
- Rasio F.A., Ford E.B., 1996, Science 274, 954
- Saar S.H., Butler R.P., Marcy G.W., 1998, ApJ 498, L153
- Sadakane K., Honda S., Kawanomoto S., et al., 1999, PASJ 51, 505
- Santos N.C., Mayor M., Naef. D., et al., 2000, A&A in press
- Schaller G., Schaerer D., Meynet G., Maeder A., 1992, A&AS 96, 269
- Schuster W.J, Nissen P.E., 1989, A&A 221, 65
- Snedden C., 1973, Ph.D. thesis, University of Texas
- Taylor B.J., 1996, ApJS 102, 105
- Tomkin J., Edvardsson B., Lambert D.L., Gustafsson B., 1997, A&A 327, 587
- Tsujiimoto T., Yoshii Y., Nomoto K., Shigeyama T., 1995, A&A 302, 704
- Udry S., Mayor M., Naef D., et al., 2000, A&A 356, 590
- Weidenshilling S.J., Marzari F., 1996, Nat 384, 619
- Wuchterl G., 1996, BAAS 28, 11.07
- Zuckerman B., Forveille T., Kastner J.H., 1995, Nat 373, 494